Article

Journal of Vibration and Control
2016, Vol. 22(5) 1244–1256

DOI: 10.1177/1077546314536427
jvc.sagepub.com

Linear matrix inequality-based robust proportional derivative control of a two-link flexible manipulator

Z Mohamed[1], M Khairudin[2], AR Husain[1] and B Subudhi[3]

Abstract

This paper presents the design and development of a robust proportional derivative (PD) controller based on linear matrix inequality (LMI) for the control of a hub angular position and end-point deflection of a planar two-link flexible manipulator. The dynamics of the manipulator is uncertain and time varying due to the variation of payloads that result in large variations in the excitation of flexible modes. Practical design steps are presented in which the LMI-based conditions are formulated to obtain a robust PD gains to control the flexible manipulator. The robust controller has an advantage as compared to the Ziegler-Nichols tuned PD controller as the identified PD gains can be used to control the system under various loading conditions. The performances of the proposed controller are evaluated in terms of input tracking capability of the hub angular position response and level of deflection of both links of the flexible manipulator. Experimental results show that despite using the same sets of PD gains, LMI-PD control provides better robustness and system performance.

Keywords

Flexible manipulator, LMI, PD control, robust control, system identification

1. Introduction

Flexible manipulators offer several advantages over rigid robots such as requiring less material, being lighter in weight, consuming less power, requiring smaller actuators, being more maneuverable and transportable and having less overall cost and a higher payload to robot weight ratio. These types of robots are used in a wide spectrum of applications starting from simple pick and place operations of an industrial robot to micro-surgery, maintenance of nuclear plants and space robotics (Dwivedy and Eberhard, 2006). However, control of flexible manipulators to maintain accurate positioning is extremely challenging. The complexity of the problem increases dramatically for a two-link flexible manipulator as the system is a class of multi-input multi-output (MIMO) system and several other factors such as coupling between both links and the effects of vibration between both links have to be considered. For single-link manipulators, linear models have been shown to be sufficient to solve the control problems. A two-link flexible manipulator, instead, necessitates more precise and complex nonlinear models, leading to complex control algorithms. Moreover, the dynamic behavior of the manipulator is significantly affected by payload variations.

As the control problem is challenging, there is a great interest in the development of control strategies for flexible manipulators. Several control strategies have been reported for control of these manipulators which include a proportional derivative (PD) controller (Choura and Yigit, 2001), optimal control (Morris and

[1]Faculty of Electrical Engineering, Universiti Teknologi Malaysia, Johor, Malaysia
[2]Department of Electrical Engineering, Universitas Negeri Yogyakarta, Indonesia
[3]Centre for Industrial Electronics and Robotics, National Institute of Technology Rourkela, India

Received: 3 November 2013; accepted: 9 April 2014

Corresponding author:
Z Mohamed, Faculty of Electrical Engineering, Universiti Teknologi Malaysia, 81310 UTM Johor Bahru, Johor, Malaysia.
Email: zahar@fke.utm.my

Madani, 1998), adaptive control (Pradhan and Subudhi, 2012), fuzzy logic control (Qiu et al., 2013) and decomposed dynamic control (Yin et al., 2013). Several robust controllers have also been proposed for control of these manipulator systems. These include a combined robust algorithm based on a sliding mode variable structure and H_∞ control (Li et al., 2000) and a robust controller using neural network-based quasi-static deflection compensation (Li et al., 2005). H_∞-based proportional-integral-derivative (PID) control has been proposed for the control of a single-link flexible manipulator (Ho and Tu, 2006).

One of the promising techniques for optimizing controller parameters is using linear matrix inequality (LMI). As LMIs can be solved numerically by using efficient standard numerical algorithms, a number of works applied these to control problems. These include development of a robust PID controller for a continuous stirred-tank reactor based on a linear quadratic regulator (LQR) and LMI approach (Ge et al., 2002), robust controller for MIMO systems (Chou et al., 2007), robust PID compensation for an inverted-cart pendulum system (Ghosh et al., 2012) and the application of LMI to design a robust decentralized controller for continuous linear time-invariant systems (Labibi et al., 2011). Besides the above, the LMI approach has been used to obtain an optimal sliding surface for sliding mode control of active magnetic bearing systems (Husain et al., 2008) and for a robust controller of boost converters (Olalla et al., 2010). A two-step design procedure for LMI-based robust PID synthesis has been proposed based on convex optimization considering the closed-loop transfer matrix and robust regional pole-placement as objective functions (Goncalves et al., 2008).

This paper presents the design and development of a robust PD controller based on LMI approach for a nonlinear two-link flexible manipulator. It is found that the LMI approach has not been explored for control of a two-link flexible manipulator where the system dynamics have uncertainties due to the variation of payloads. Using the robust controller, identified PD gains can be used for all payloads with satisfactory responses. This is an advantage as compared to Ziegler-Nichols (ZN) tuned PD control which needs to be re-tuned for different payloads. The ZN tuning method is a standard procedure for the tuning of PID controller parameters. To cast this control design problem into the LMI framework, the transfer functions of the system with various payloads are obtained by carrying out system identification. Subsequently, the dynamic model is represented into convex formulation which leads to the formulation of system requirement into LMIs representation that can accommodate the convex model. A set of robust PD gains is then obtained by solving the LMIs with desired specifications. For performance assessment, LMI-PD and ZN-PD controllers are compared for control of the manipulator in terms of input tracking, deflection reduction level and robustness to payload variations of both links. Experimental results show that better robustness and system performance are achieved with LMI-PD controller despite using a single set of PD gains.

2. The two-link flexible manipulator

Figure 1 shows the experimental setup of a two-link flexible manipulator used in this work. The rig consists of three main parts: a two-link flexible arm, sensors and a processor. The flexible links are constructed using a piece of thin aluminum with specifications as given in Table 1. The links are cascaded in a serial fashion and are actuated by rotors and hubs with individual motors. l_1 and l_2 denote link lengths of uniform mass density

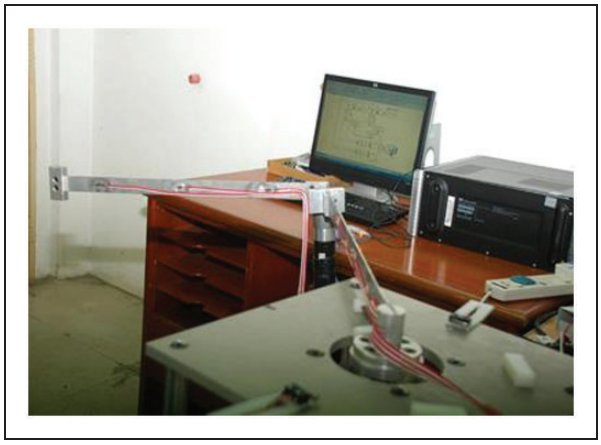

Figure 1. The experimental setup of a two-link flexible manipulator.

Table 1. Parameters of a two-link flexible manipulator.

Symbol	Parameter	Link-1	Link-2	Unit
m_1, m_2	Mass of link	0.08	0.05	kg
ρ	Mass density	2666.67	2684.56	kgm^{-1}
EI	Flexural rigidity	1768.80	597.87	Nm^2
J_{h1}, J_{h2}	Motor and hub inertia	1.46×10^{-3}	0.60×10^{-3}	kgm^2
l_1, l_2	Length of link	0.5	0.5	m
	Width of link	0.03	0.025	m
	Thickness of link	2×10^{-3}	1.49×10^{-3}	m
J_{01}, J_{02}	Moment of inertia	5×10^{-3}	3.125×10^{-3}	kgm^2
M_{h2}	Mass of the center rotor	–	0.155	kg

per unit length ρ_1 and ρ_2. The first link is clamped at the rotor of the first motor whereas the second motor is attached at the tip of the first link. E and I represent the Young's modulus and area moment of inertia of both links respectively. There is a provision for attaching payloads at the end-point of link-2.

The sensors used in the system are shaft encoders at the motors and strain gauges placed along the arms. Two encoders, HEDL-5540 and HEDS-5540 (Maxon Motor Ag Corporation, 2003) with 500 counts per revolution are used to measure the angular positions of link-1 and link-2 respectively. A precision interface circuit consisting of PCIQUAD04 with four input channels has been constructed for measurement and interfacing with a real-time system. On the other hand, the strain gauges are used for measurement of deflections of the links.

MATLAB Real-time toolbox is used for real-time interfacing and control of the system. Data acquisition and control are accomplished by employing a PCI6221 I/O board that provides a direct interface between the processor, actuators and sensors through signal conditioning circuits SCC-AI for analogue input, SCC-AO for analogue output and SCC-SG for strain gauges. The experimental rig requires two-analogue outputs for both motors and four analogue inputs from the encoders and strain gauges for both links.

3. Dynamic model

Modeling of a two-link flexible manipulator resulted in nonlinear dynamic equations of motion as detailed in Khairudin el al. (2010). Due to high nonlinearity of the dynamic model, formulation of a robust control algorithm is difficult, and thus a simple and practical method is required. Moreover, control of the nonlinear and high complexity model control design methods often require excessive computational time. In this study, formulation of a robust control method is based on a set of linear models which closely represent the nonlinear model of a two-link flexible manipulator. This is obtained by carrying out system identification under various system payloads which further leads to a much simpler controller, yet capable of achieving various system requirements.

Using the system identification technique, a set of linear models of the two-link flexible manipulator that represents the operating ranges of the dynamic system is obtained. A multisine signal that produces sinusoids of different amplitudes and frequencies, and can be summed to constitute a persistent excitation signal is used in the identification process. The signals are carefully adjusted to provide very low speed operation, which is essential for examination of the system nonlinearities. Figure 2 shows the multisine signal applied to both links.

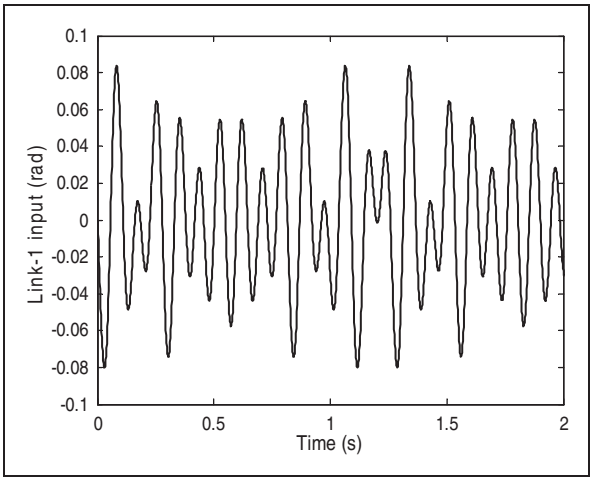

Figure 2. A multisine input signal.

The data of stimulation and response is acquired with a sampling time of 0.001 s and system identification is performed using MATLAB to obtain a linear model of the system. An ARX model structure is considered and the least square technique is applied to identify the parameters of the transfer function model. In this work, the model structure $G(z) = B(z)/A(z)$ is used where $B(z)$ and $A(z)$ are numerator and denominator of the system transfer function in discrete time. The system's transfer function in continuous time is then obtained using MATLAB. Investigations for the system without payload, and payloads of 50 g and 100 g are performed. For the system without payload, a sixth-order identified model of link-1 that relates the hub angular position output to the voltage input is obtained as

$$G_{11}(s) = \frac{\left\{ \begin{array}{c} -58.9\,s^5 - 807\,s^4 - 3301.1\,s^3 - 3330\,s^2 \\ +1991.8\,s + 3605.9 \end{array} \right\}}{\left\{ \begin{array}{c} s^6 + 21.7\,s^5 + 196\,s^4 + 926.9\,s^3 \\ +2261.3\,s^2 + 2292.1\,s + 704 \end{array} \right\}} \quad (1)$$

where s is a Laplace operator, the first subscript represents link-1 and the second subscript shows the load condition 1. On the other hand, the transfer function for link-2 is obtained as

$$G_{21}(s) = \frac{\left\{ \begin{array}{c} -84.1\,s^5 - 840.9\,s^4 - 2571.1\,s^3 \\ -2782.5\,s^2 - 1080.3\,s - 91.2 \end{array} \right\}}{\left\{ \begin{array}{c} s^6 + 10.9041\,s^5 + 50.9482\,s^4 + 113.1691\,s^3 \\ +112.1175\,s^2 + 47.4569\,s + 6.8364 \end{array} \right\}} \quad (2)$$

The same procedures are adopted to obtain transfer functions of the flexible manipulator with payload. With a payload of 50 g, the transfer function for link-1 is obtained as

$$G_{12}(s) = \frac{\left\{ \begin{array}{c} -19.27\,s^5 - 175.63\,s^4 - 432.35\,s^3 \\ -40.68\,s^2 + 600.68\,s + 372.67 \end{array} \right\}}{\left\{ \begin{array}{c} s^6 + 14.49\,s^5 + 86.87s^4 + 279.78\,s^3 \\ +499.53\,s^2 + 443.88\,s + 150.46 \end{array} \right\}} \quad (3)$$

and link-2 as

$$G_{22}(s) = \frac{\left\{ \begin{array}{c} -68.6\,s^5 - 601.7\,s^4 - 2011.7\,s^3 \\ -3142.4\,s^2 - 2190.6\,s - 517.5 \end{array} \right\}}{\left\{ \begin{array}{c} s^6 + 9.557\,s^5 + 40.0934\,s^4 + 87.9419\,s^3 \\ +94.5527\,s^2 + 45.5913\,s + 7.9146 \end{array} \right\}} \quad (4)$$

On the other hand, with a payload of 100 g, the transfer function for link-1 can be found as

$$G_{13}(s) = \frac{\left\{ \begin{array}{c} -65.6\,s^5 - 455.6\,s^4 - 1304.6\,s^3 \\ -1736\,s^2 + 1236.8\,s + 2146.2 \end{array} \right\}}{\left\{ \begin{array}{c} s^6 + 14.05\,s^5 + 86.42\,s^4 + 292.02\,s^3 \\ +550.57\,s^2 + 530.97\,s + 199.19 \end{array} \right\}} \quad (5)$$

and the transfer function for link-2 as

$$G_{23}(s) = \frac{\left\{ \begin{array}{c} -98.7\,s^5 - 1005.9\,s^4 - 3596.7\,s^3 \\ -5434.3\,s^2 - 3678.6\,s - 938.5 \end{array} \right\}}{\left\{ \begin{array}{c} s^6 + 10.6392\,s^5 + 50.2485\,s^4 + 122.9197\,s^3 \\ +152.7299\,s^2 + 89.9483\,s + 19.6417 \end{array} \right\}} \quad (6)$$

Comparison of the responses to the multisine input signal obtained using the linear models and actual system reveal that all the transfer functions of the flexible manipulator have a matching degree of at least 94%. Thus, confidence in utilizing the identified models has been established. On the design of the LMI robust controller, the transfer functions are converted into state-space forms. Subsequently, the models are used in the development of ZN-PD and LMI-PD controllers.

4. Design of linear matrix inequality (LMI)-based robust proportional derivative (PD) controller

In this work, the LQR approach is considered as a basis for determining the PD controller gains since this approach can provide a high degree of robustness and design flexibility. Moreover, it can be formulated in term of a performance-based optimization problem which can be solved using a numerical technique (Ge et al., 2002). To ensure that the approach is applicable simultaneously to the set of multiple linear models, the LQR problem needs to be represented in term of LMI sets for finding the common Lyapunov function for the set of particular linear models. The solution of the linear model involves a form of quadratic Lyapunov function that not only gives the stability of the closed-loop control system but can also be used to achieve certain desired performance specifications.

4.1. Robust proportional derivative (PD) controller design

Most of the existing PD tuning methods were developed with few robustness features. Since a robust controller is required to control a two-link flexible manipulator under various payload conditions, a robust PD controller design is proposed in this work.

Consider an uncertain sixth-order system for link-1 and link-2 as

$$G(s) = \frac{n_1 s^5 + n_2 s^4 + n_3 s^3 + n_4 s^2 + n_5 s + n_6}{s^6 + d_1 s^5 + d_2 s^4 + d_3 s^3 + d_4 s^2 + d_5 s + d_6} \quad (7)$$

where the parameter vary in intervals

$$\begin{aligned} d_1 &\in \left[\underline{d_1}, \overline{d_1}\right], \ldots\ldots, d_6 \in \left[\underline{d_6}, \overline{d_6}\right], \\ n_1 &\in \left[\underline{n_1}, \overline{n_1}\right], \ldots\ldots, n_6 \in \left[\underline{n_6}, \overline{n_6}\right] \end{aligned} \quad (8)$$

and $\underline{d_i}$, $\overline{d_i}$ and $\underline{n_i}$, $\overline{n_i}$ are lower and upper bounds for the uncertain parameters of denominator and numerator of the system respectively.

The objective of the PD controller design is to determine PD gains to meet various design specifications. The PD controller is designed in the state-space settings for ease in using the LMI approach. The flexible link can be conveniently represented as a feedback system and it can be expressed in the state-space description as

$$\begin{aligned} \dot{x}_p(t) &= \overline{A}_p x_p(t) + \overline{B}_p u_p(t) \\ y_p &= \overline{C}_p x_p(t) \end{aligned} \quad (9)$$

where

$$\overline{A}_p = A_{p1} + \delta A_p,\ \overline{B}_p = B_{p1} + \delta B_p \text{ and } \overline{C}_p = C_{p1} + \delta C_p \quad (10)$$

For p-th link. u_p and y_p are the reference input and output respectively, $x = \begin{bmatrix} x_1 & x_2 & x_3 & x_4 & x_5 & x_6 \end{bmatrix}^T$ are the states variables, $A \in R^{6\times 6}$, $B \in R^{6\times 1}$ and $C \in R^{1\times 6}$ are system, input and output matrices

respectively. A_{p1}, B_{p1} and C_{p1} are the nominal matrices representing the system without payload. State-space representations of link-1 (A_{1q}, B_{1q}, C_{1q}) and link-2 (A_{2q}, B_{2q}, C_{2q}) of the flexible manipulator represent cases without payload, 50 g payload and 100 g payload respectively where $q = 1$, 2 and 3. δA_p, δB_p and δC_p are matrices of uncertainties of the respective dimensions. The uncertainties are considered to be in the form of

$$\begin{aligned} &\delta A_p = \varepsilon_1 A_{p2} + \varepsilon_2 A_{p3}, \quad \delta B_p = \varepsilon_1 B_{p2} + \varepsilon_2 B_{p3}, \\ &\delta C_p = \varepsilon_1 C_{p2} + \varepsilon_1 C_{p3} \end{aligned} \tag{11}$$

where ε_1 and ε_2 are uncertainty parameters either -1 or 1. The feedback control law is considered in the form of

$$u_p(t) = F_p \overline{C}_{pj} x_p(t) \tag{12}$$

where F_p is a matrix corresponding to the controller. The LQR approach is used to design the state feedback controller, however, for LQR design the response rate or overshoot is often limited. To accommodate the design specification, an additional derivative term is included in the cost function containing state variables to explore the possibility of damping the oscillations and limiting the response rate. The function can be represented as

$$J_p = \int_0^\infty \left[x_p(t)^T Q x_p(t) + u_p(t)^T R u_p(t) + \dot{x}_p(t)^T S \dot{x}_p(t) \right] \mathrm{d}t \tag{13}$$

where Q, S and R are symmetric positive definite matrices. The objective is to develop a PD control algorithm that stabilizes the uncertain system in equation (9) with respect to the cost function shown in equation (13). However, with the introduction of the derivative term, the controller in equation (12) needs to be augmented to accommodate the closed-loop system design such that

$$u_p(t) = F_p \overline{C}_{pj} x_p(t) + F_{dp} C_{dp} \dot{x}_p(t) \tag{14}$$

where $F_p \overline{C}_{pj} x_p(t)$ and $F_{dp} C_{dp} \dot{x}_p(t)$ are the proportional and derivative terms of the PD controller respectively.

The resulting closed-loop system with the PD controller in equation (14) can be obtained as

$$\dot{x}_p = \overline{A}_{pj} x_p(t) + \overline{B}_{pj} \left(F_p \overline{C}_{pj} x_p(t) + F_{dp} C_{dp} \dot{x}_p(t) \right) \tag{15}$$

where $j = 1$, 2 and 3 represent cases without payload, 50 g payload and 100 g payload respectively. Equation (15) can be represented as

$$\dot{x}_p(t) = \hat{A}_p x_p(t) + \overline{B}_{pj} F_{dp} C_{dp} \dot{x}_p(t) \tag{16}$$

where

$$\hat{A}_p = \left(\overline{A}_{pj} + \overline{B}_{pj} F_p \overline{C}_{pj} \right) \tag{17}$$

F_p and F_{dp} are proportional and derivative gains respectively. In practical situations, the controller needs to meet various specifications simultaneously and the design specifications are often a mixture of performance and robustness objectives.

4.2. Linear matrix inequality-based robust proportional derivative controller

The concept of LMI and the constraints used in the controller synthesis problem for design of the robust PD controller is presented in this section. The standard LQR problem is to determine the control signal u which minimizes the quadratic cost function. The cost function in equation (13) can be expressed as

$$J_p = \int_0^\infty \begin{bmatrix} x_p^T & \dot{x}_p^T \end{bmatrix} \overline{Q} \begin{bmatrix} x_p \\ \dot{x}_p \end{bmatrix} \mathrm{d}t \tag{18}$$

where

$$\overline{Q} = \begin{bmatrix} Q + \overline{C}_{pj}^T F_p^T R F_p \overline{C}_{pj} & 0 \\ 0 & S \end{bmatrix}.$$

Define that the matrix

$$\begin{bmatrix} x_p^T & \dot{x}_p^T \end{bmatrix} \begin{bmatrix} Q + \overline{C}_{pj}^T F_p^T R F_p \overline{C}_{pj} & X_p \\ X_p & S \end{bmatrix} \begin{bmatrix} x_p \\ \dot{x}_p \end{bmatrix} < 0 \tag{19}$$

where X_p is a symmetric positive definite matrix. However, in order to solve for the cost function in equation (18), it is defined such that

$$\hat{J}_p \leq x_p^T(0) X_p x_p(0) \tag{20}$$

where $\hat{J}_p$ is a guaranteed cost value and $x_p(0)$ is initial condition for x_p.

An efficient alternative for solving the LQR problem is to exploit the LMI technique that has emerged recently as a powerful design utility for a variety of control problems due to its convexity. Define design matrices H_p and G_p of appropriate dimensions, equation (16) can be written as

$$\begin{aligned} &\left(-x_p^T H_p - \dot{x}_p^T G_p^T \right) \left(\dot{x}_p - \hat{A}_p x_p - \overline{B}_{pj} F_{dp} C_{dp} \dot{x}_p \right) \\ &\quad + \left(\dot{x}_p - \hat{A}_p x_p - \overline{B}_{pj} F_{dp} C_{dp} \dot{x}_p \right)^T \left(H_p^T x_p - G_p \dot{x}_p \right) = 0 \end{aligned} \tag{21}$$

Using Schur complements (Boyd et al., 1994), equation (21) can be written as

$$\begin{bmatrix} x_p^T & \dot{x}_p^T \end{bmatrix} P \begin{bmatrix} x_p \\ \dot{x}_p \end{bmatrix} < 0 \tag{22}$$

where

$$P = \begin{bmatrix} \begin{pmatrix} -\hat{A}_p^T H_p^T + H_p \hat{A}_p + \\ Q + \overline{C}_{pj}^T F_p^T R F_p \overline{C}_{pj} \end{pmatrix} & \begin{pmatrix} X_p - H_p \begin{pmatrix} I - \\ \overline{B}_{pj} F_{dp} C_{dp} \end{pmatrix} + \hat{A}_p^T G_p \end{pmatrix} \\ \begin{pmatrix} X_p + \left(I - C_{dp}^T F_{dp}^T \overline{B}_{pj}^T\right) H_p^T \\ + G^T \hat{A}_p \end{pmatrix} & \begin{pmatrix} -\left(I - C_{dp}^T F_{dp}^T \overline{B}_{pj}^T\right) G_p - \\ G_p^T \left(I - \overline{B}_{pj}^T F_{dp} C_{dp}\right) + S) \end{pmatrix} \end{bmatrix}$$

There exist matrices X_p, H_p, G_p, F_p and F_{dp} of the respective dimensions such that

$$\begin{bmatrix} -\hat{A}_p^T H_p^T + H_p \hat{A}_p + Q & X_p - H_p M_{dp} + \hat{A}_p^T G_p \\ + \overline{C}_{pj}^T F_p^T R F_p \overline{C}_{pj} & \\ X_p + M_{dp}^T H_p^T + G_p^T \hat{A}_p & -M_{dp}^T G_p - G_p^T M_{dp} + S \end{bmatrix} < 0 \tag{23}$$

where

$$M_{dp} = (I - \overline{B}_{pj} F_{dp} C_{dp}) \tag{24}$$

It is noted that M_{dp} includes the derivative part of the PD controller.

To obtain a solution of LMIs in equation (23) all over the uncertain system will obviously be an arduous task. However, since the uncertainties of the system can be described as a set polytopic uncertainty (Boyd et al., 1994; Ge et al., 2002), solutions can be sought only at the polytopic vertices instead of all points within the polytope. Therefore, a solution to LMIs in equation (23) can be obtained and the task for solving the constraint becomes simpler. The advantage of using LMI is its flexibility of including other specifications future system needs in the design. Therefore, various design specifications may be recast into the LMIs and the resulting LMI constraints can be efficiently solved in polynomial time by using convex optimization algorithms (Gahinet and Apkarian, 1994).

It is a desirable property of the closed-loop system that its poles are located in a certain region of the complex plane to ensure some desired dynamical properties such as overshoot and settling time are achieved. A region of the complex plane $S(\alpha, d, \vartheta)$ has been proposed (Chilali and Gahinet, 1996) where α, d and ϑ are minimum decay rate, the length of disk and inner angle respectively, as depicted in Figure 3. The poles of the system are defined in the form $x \pm yi$ that satisfy

$$|x \pm yi| \le d, \quad x \le \alpha \quad \text{and} \quad y \le (\tan(\vartheta))d \tag{25}$$

where $\alpha = 0$. A pole-placement region to achieve control objectives will be determined and used in designing an LMI-PD controller.

5. Controller implementation

Figure 4 shows a block diagram of the PD controllers for position control of link-1 and link-2 of a flexible manipulator where θ_{1r} and θ_{2r} are desired hub angular positions for link-1 and link-2 respectively and θ_1 and θ_2 are actual hub angular positions for both links. For such a MIMO system, two PD controllers are required for both links. Essentially, the task of these controllers is to position both links of the flexible manipulator to a

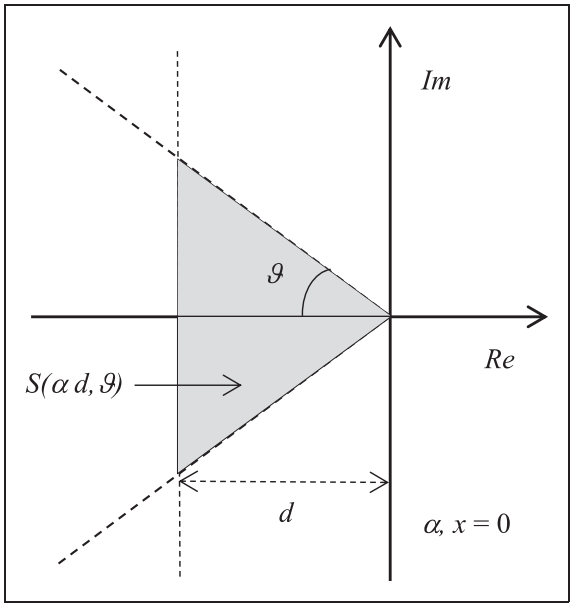

Figure 3. Pole-placement region.

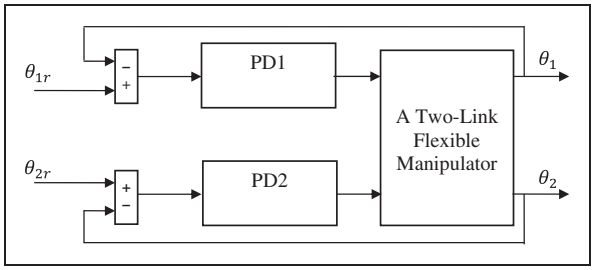

Figure 4. A block diagram of the closed-loop system with proportional derivative (PD) controllers.

Table 2. Proportional derivative parameters obtained using Ziegler-Nichols technique.

	Link-1		Link-2	
Payload (g)	F_1	F_{d1}	F_2	F_{d2}
0	0.1410	0.3591	0.1055	0.3122
50	0.1468	0.3632	0.1083	0.3200
100	0.1493	0.3675	0.1100	0.3285

specified commanded position. The hub angular positions of both links are fed back and used to control the flexible manipulator. Step signals with amplitudes of -0.5 rad and 0.35 rad are used as reference inputs for hub angular positions of link-1 and link-2 respectively. Two system responses, namely the hub angular positions and deflections with the frequency response of the deflections, are obtained and evaluated. The control objective is to achieve the desired hub angular position with low deflection. It is desirable to have a uniform performance for all payload conditions.

For performance assessment of the robust controller, a ZN-PD controller is designed where the tasks are to find two sets of PD controller gains for hub angular position control of link-1 and link-2 of the flexible manipulator. In this work, the ZN closed-loop method is considered for the tuning of PD parameters. As a ZN-PD controller can only provide an optimum response for a certain payload, different sets of PD gains have to be calculated for each loading condition considered in this work. By carrying out the ZN closed-loop tuning method with the flexible manipulator without payload and payloads of 50 g and 100 g, PD controller gains are obtained as listed in Table 2.

The flow chart shown in Figure 5 is adopted to develop the LMI-PD controller. Based on several investigations, $Q = 0.25 * I_{6\times6}$, $R = [1]$ and $S = 1 \times 10^{-6} * I_{6\times6}$ are deduced for control of the system. By carrying out the steps in the flowchart, 64 combinations of uncertain systems are obtained with their respective PD gains, F_p and F_{dp} gains. Based on an application for control of the two-link flexible manipulator and multivariable system, the robust PD controller is designed with the pole-placement parameters, $\alpha < 0$, $d = -8$ and $\vartheta = 30$ degrees within the pole-placement region (Chilali and Gahinet, 1996). This implies that the desired minimum closed-loop eigenvalue is located at $-8 \pm 4.6188\,i$. Based on the 64 polytopic models and the pole-placement region constraint, $F_1 = 0.1225$ and $F_{d1} = 0.2235$ are obtained as the PD gains for control of link-1 of the manipulator and $F_2 = 0.0961$ and $F_{d2} = 0.2023$ for link-2. By using the gains, closed-loop eigenvalues of the system are achieved within the desired region. With the proposed robust controller, only a single set of PD gains is needed to control the system under various loading conditions. This is clearly an advantage as compared to the ZN-PD controller.

6. Experimental results

Experimental results of the LMI-PD and ZN-PD controllers implemented on the experimental two-link flexible manipulator are presented in this section. The task of these controllers is to position hub angles of link-1 and link-2 of the manipulator at −0.5 rad and 0.35 rad respectively. For real-time implementation of both controllers, Real-time Windows Target in MATLAB and Simulink environment are utilized.

6.1. System without payload

Figure 6 shows the hub angular position responses of the experimental two-link flexible manipulator without payload for both links with the LMI-PD and ZN-PD controllers. Both techniques are able to meet the desired angular positions of −0.5 rad and 0.35 rad for link-1 and link-2 respectively. However, it is noted that the system with LMI-PD control exhibits faster settling times for both links as compared to ZN-PD. Moreover, with LMI-PD control, smoother responses with no overshoot are observed and the settling times are almost 30% faster than the results with ZN-PD for both links. Deflection responses of link-1 and link-2 with both controllers are shown in Figure 7 where the magnitude of deflections with LMI-PD is lower as compared to the results with ZN-PD control. With the robust LMI-PD controller, the maximum magnitudes of deflection are 3.36 mm and 2.21 mm for link-1 and link-2 respectively whereas using ZN-PD as 7.50 mm and 5.00 mm. Moreover, the deflections with the robust controller converge to zero faster than the response with the ZN-PD control.

Figure 8 shows the frequency response of the deflection obtained with both controllers. In this work, the first mode of vibration is considered as this is the most dominant mode that characterizes dynamics of the

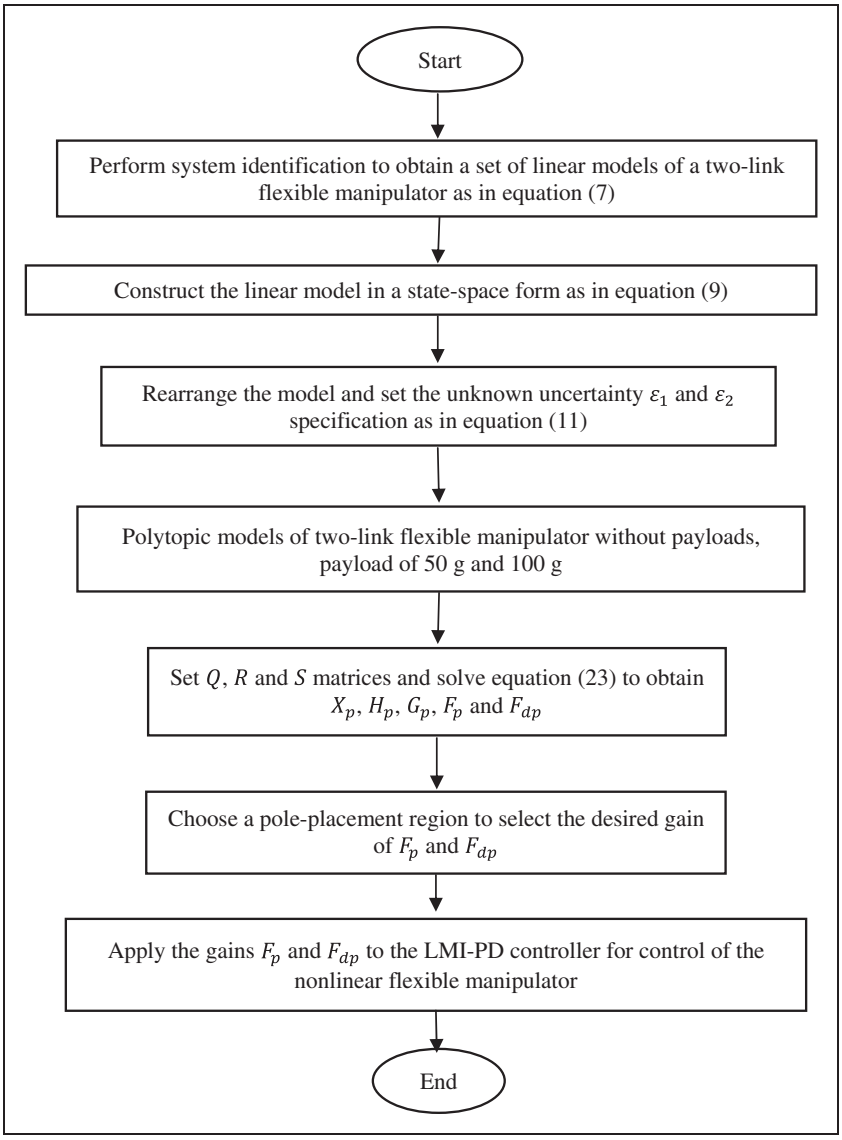

Figure 5. Flow chart to develop and implement the linear matrix inequality (LMI)-proportional derivative (PD) controller.

deflection. It is shown that the level of deflections with the LMI-PD control is 8.59 dB and 6.91 dB lower than the response with the ZN-PD control for link-1 and link-2 respectively. This proves that the robust LMI-PD controller yields lower deflections.

6.2. System with payload

To assess the robustness performance of the controllers, the flexible manipulator with payloads of 50 g and 100 g is examined. For the ZN-PID controller, the PD gains given in Table 2 are used with the respective payloads whereas similar PD gains are used for the LMI-PID control. Figure 9 shows hub angular position responses of link-2 of the flexible manipulator when it is subjected with payloads of 50 g and 100 g, using both controllers. Despite varying payloads, both techniques are able to meet the desired angular position of 0.35 rad. Similar to the case without payload, the LMI-PD control has resulted in faster settling times as compared to the ZN-PD control. In addition with the LMI-PD control, no overshoot is observed. Table 3 summarizes the settling times and overshoots yielded with the application of the controllers for both the links. Figure 10 shows the deflection responses of link-2 while, by copying payloads of 50 g and 100 g, using both controllers. Similar to the case without payload, the robust LMI-PD controller yielded a smaller deflection as compared to the results with ZN-PD control for both payloads. Table 4 summarizes the maximum magnitude of the responses

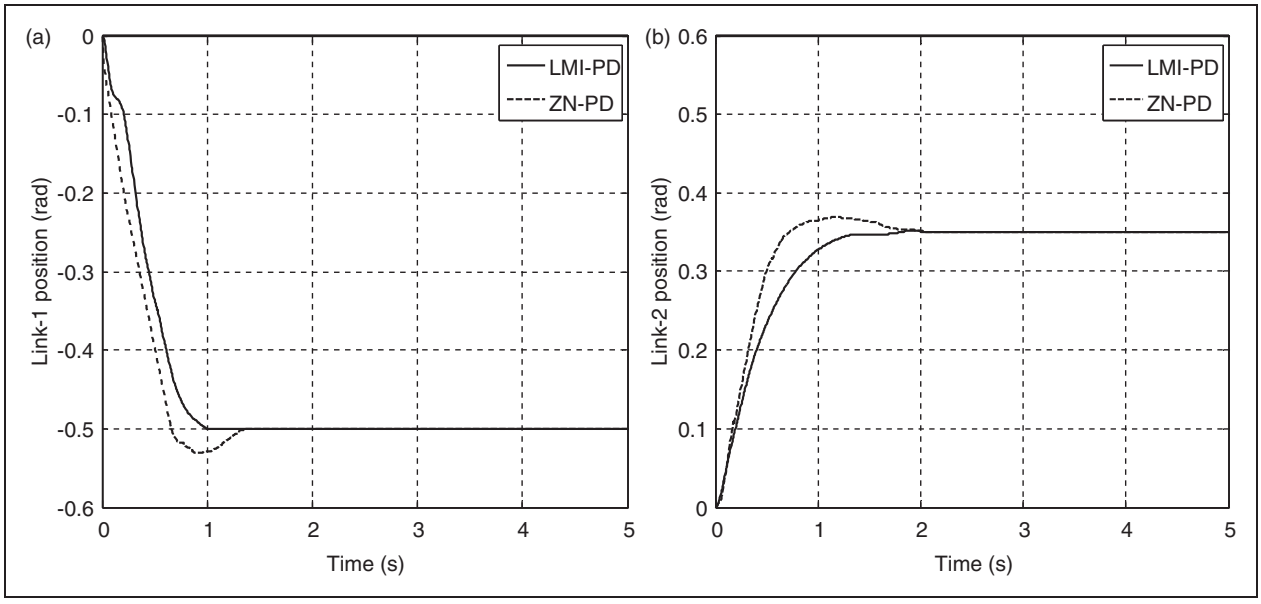

Figure 6. Angular position response of the experimental rig without payload (a) Link-1; (b) Link-2.

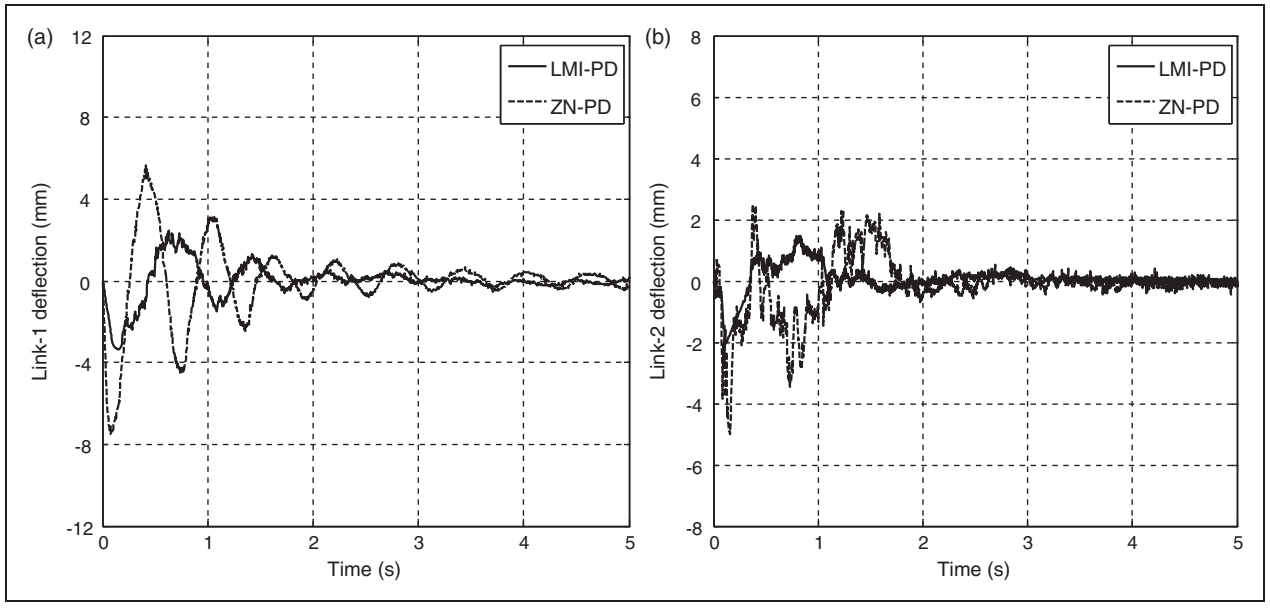

Figure 7. Deflection response of the experimental rig without payload (a) Link-1; (b) Link-2.

for link-1 and link-2 obtained with the LMI-PD control and ZN-PD control. For all cases, it is noted that maximum deflections with the LMI-PD control is reduced to almost half of the deflection with ZN-PD control. Moreover, the deflections converge to zero faster with the LMI-PD control.

Figure 11 shows the frequency response of the deflection of link-2 obtained with both controllers for the manipulator with both payloads. Similarly, the deflection amplitude yielded with the LMI-PD is less as compared to with ZN-PD control. It is also noted that the deflection with LMI-PD control is 9.22 dB and 11.84 dB lower than with the ZN-PD control for payloads of 50 g and 100 g respectively.

The robust LMI-PID controller is designed to control the flexible manipulator with a payload in a range of 0–100 g. Figures 6–11 show that the proposed robust controller provides satisfactory results and performs better than ZN-PID control for the system without and with payloads of 50 g and 100 g. However, as the

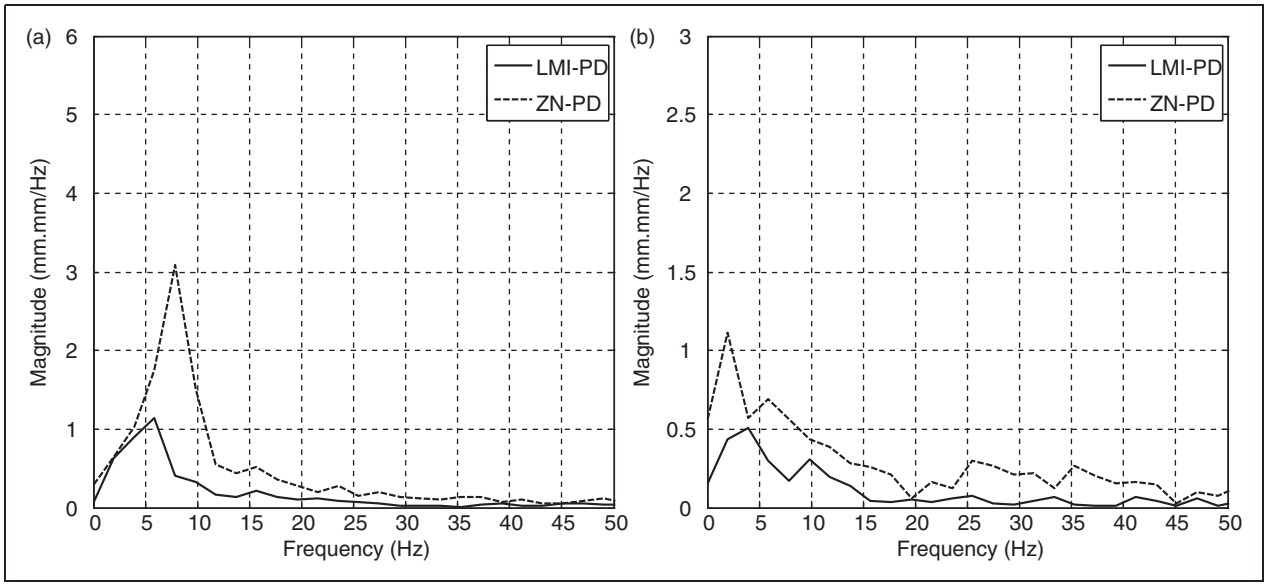

Figure 8. Frequency response of deflection of the experimental rig without payload (a) Link-1; (b) Link-2.

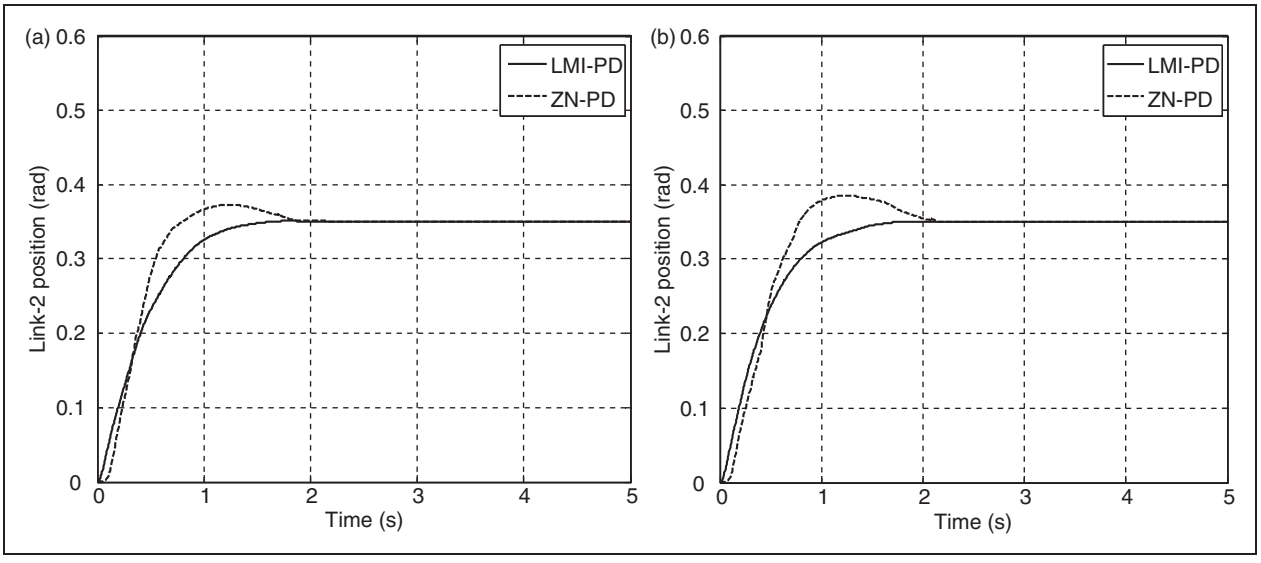

Figure 9. Angular position response of link-2 of the experimental rig with payloads of 50 g and 100 g (a) 50 g; (b) 100 g.

Table 3. Specification of angular position response of the flexible manipulator with various payloads.

	Link-1				Link-2			
	Settling time (s)		Overshoot (%)		Settling time (s)		Overshoot (%)	
Payload (g)	LMI-PD	ZN-PD	LMI-PD	ZN-PD	LMI-PD	ZN-PD	LMI-PD	ZN-PD
0	0.90	1.24	0.00	3.68	1.17	1.61	0.00	7.11
50	0.96	1.72	0.00	9.12	1.24	1.69	0.00	8.57
100	1.02	1.77	0.00	9.52	1.36	1.80	0.01	10.86

LMI-PD: linear matrix inequality-proportional derivative; ZN-PD: Ziegler-Nichols-proportional derivative.

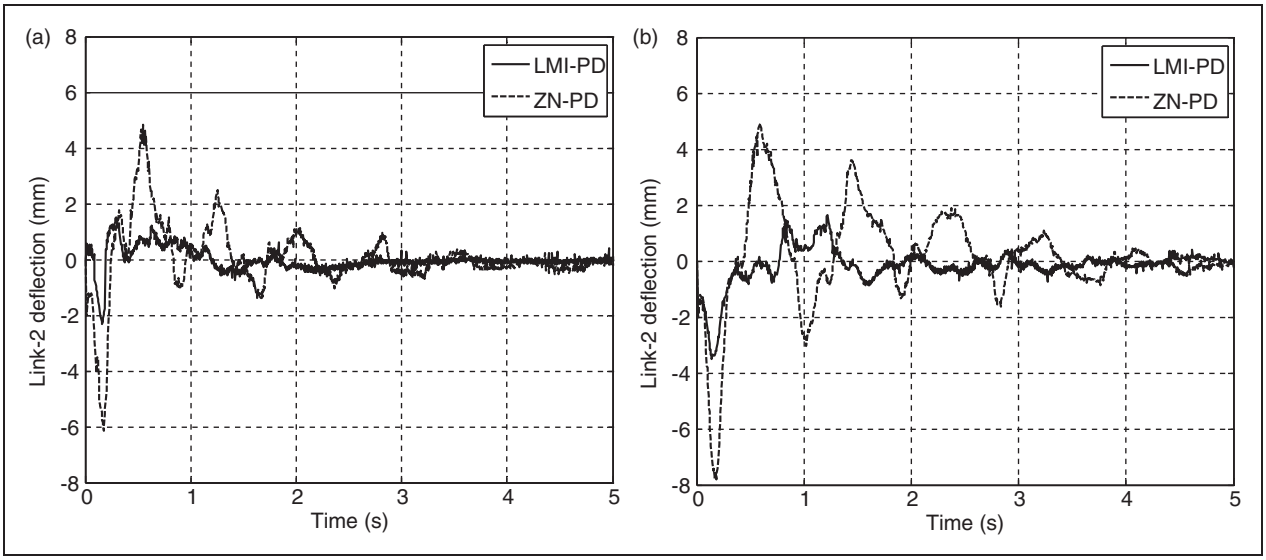

Figure 10. Deflection response of link-2 of the experimental rig with payloads of 50 g and 100 g payload (a) 50 g; (b) 100 g.

Table 4. Maximum magnitudes of deflection responses of the flexible manipulator with linear matrix inequality-proportional derivative and Ziegler-Nichols-proportional derivative controllers.

	Link-1		Link-2	
Payload (g)	LMI-PD (mm)	ZN-PD (mm)	LMI-PD (mm)	ZN-PD (mm)
0	3.36	7.50	2.21	5.00
50	3.37	7.62	2.33	6.16
100	3.50	7.83	3.53	7.82

LMI-PD: linear matrix inequality-proportional derivative.; ZN-PD: Ziegler-Nichols-proportional derivative.

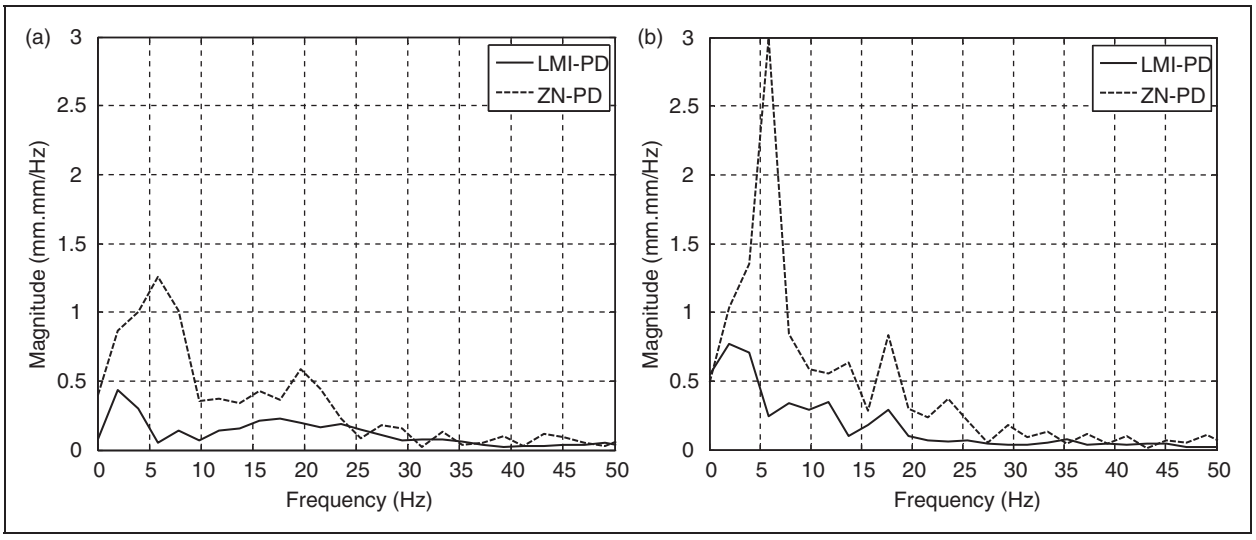

Figure 11. Frequency response of deflection of link-2 of the experimental rig with payloads of 50 g and 100 g (a) 50 g, (b) 100 g.

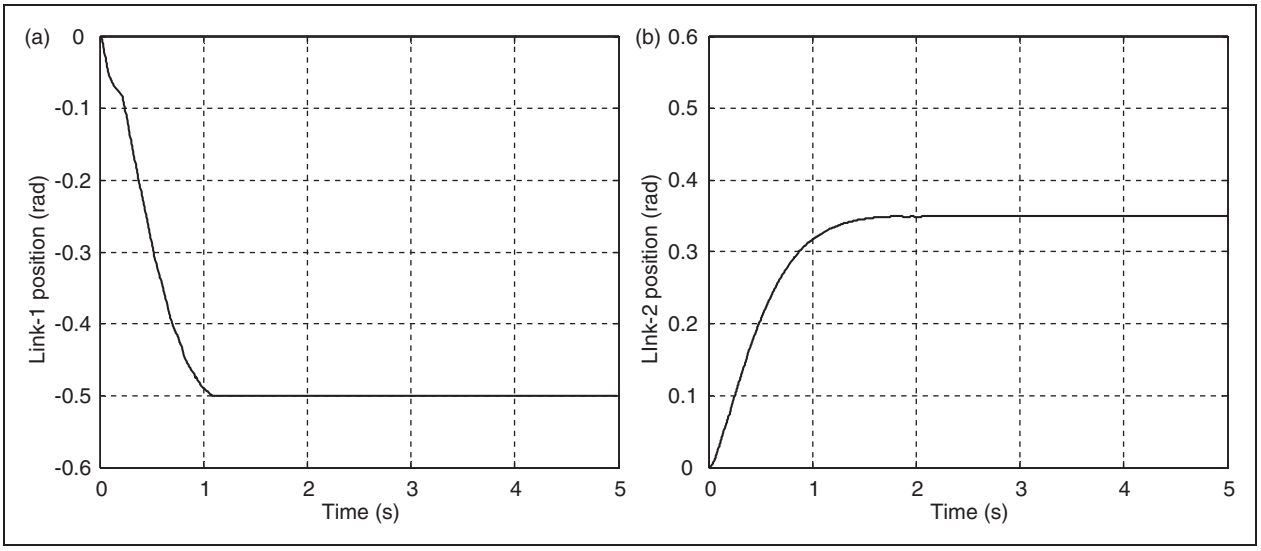

Figure 12. Angular position response of the experimental rig with 70 g payload (a) Link-1; (b) Link-2.

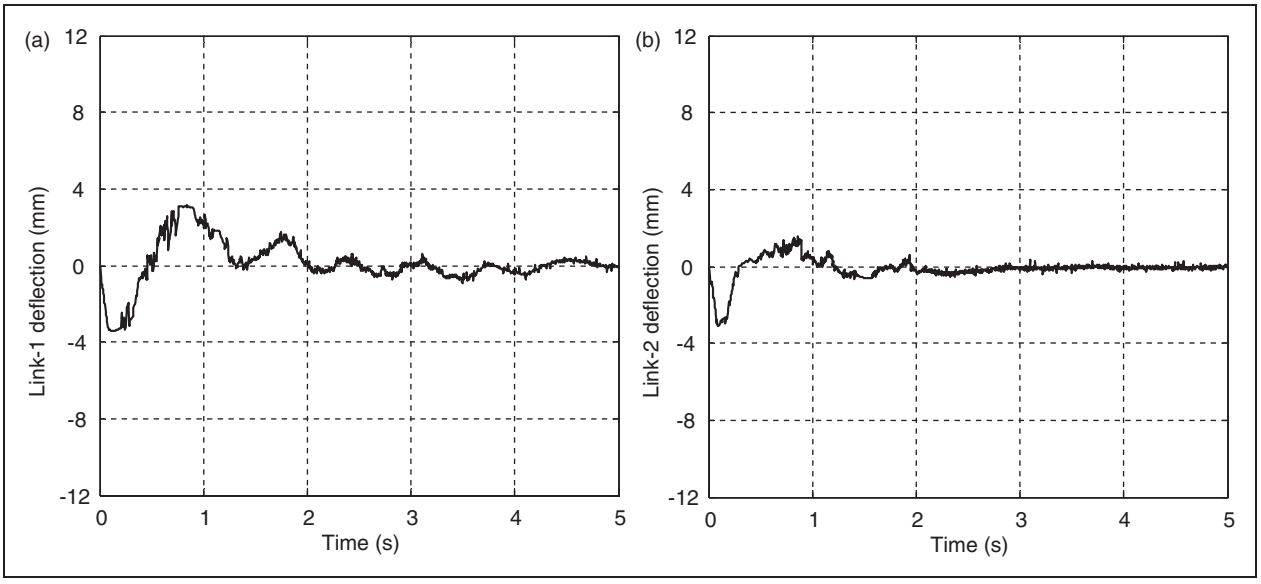

Figure 13. Deflection response of the experimental rig with 70 g payload (a) Link-1; (b) Link-2.

three cases above are used in control design and setting the lower and upper bounds of the robust controller, it is desirable to verify the performance of the LMI-PID controller with a different payload. For verification, a flexible manipulator when it carries 70 g payload is examined. Figures 12 and 13 show the hub angular position and deflection responses of the manipulator with 70 g payload respectively, using the LMI-PD control. The same PD gains as in the previous cases are used. It is shown that the desired angular positions of −0.5 rad and 0.35 rad are achieved with settling times of 1.01 s and 1.32 s for link-1 and link-2 respectively, and no overshoot is observed for both links. Low deflections for both links as in the previous cases with other payloads are also noted. In this case, the maximum magnitudes for link-1 and link-2 are 3.43 mm and 3.11 mm respectively. Thus, it was verified experimentally, that for the flexible manipulator under various payload conditions, despite using the same PD gains, a uniform system performance is achieved with the robust LMI-PD controller. Note that by extensive efforts in tuning the ZN-PD controller, similar results

as the LMI-PD control could be achieved. However the process is difficult and has to be performed for each loading condition.

7. Conclusion

The development of a robust PD control of a two-link flexible manipulator based on the LMI approach has been presented. Practical design steps have been presented where the LMI approach has been employed to obtain robust PD gains to control the flexible manipulator under various payload conditions. Robustness in the performance of the controller has been evaluated in terms of input tracking capabilities and deflections of both links of the flexible manipulator. Experimental results envisaged that despite using the same sets of PD gains, the proposed LMI-PD control provides better control performance as compared to the ZN-PD controller. Similar results as the LMI-PID controller could be obtained by extensive effort in tuning the ZN-PID controller, however this requires laborious tuning effort for each loading condition.

Funding

This research received no specific grant from any funding agency in the public, commercial, or not-for-profit sectors.

References

Boyd S, Ghaoui LE, Feron E and Balakrishnan V (1994) *Linear Matrix Inequalities in Systems and Control Theory*. Philadelphia PA: SIAM.

Chilali M and Gahinet P (1996) H_∞ design with pole placement constraints: an LMI approach. *IEEE Transactions on Automatic Control* 41: 358–367.

Chou YS, Leu JL and Chu YC (2007) Stable controller design for MIMO systems: an LMI approach. *IET Control Theory and Applications* 1: 817–829.

Choura S and Yigit AS (2001) Control of a two-link rigid-flexible manipulator with a moving payload mass. *Journal of Sound and Vibration* 243: 883–897.

Dwivedy SK and Eberhard P (2006) Dynamic analysis of flexible manipulators, a literature review. *Mechanism and Machine Theory* 41: 749–777.

Gahinet P and Apkarian P (1994) A linear matrix inequalities approach to H_∞ control. *International Journal of Robust and Nonlinear Control* 4: 421–448.

Ge M, Ciu MS and Wang QG (2002) Robust PID controller design via LMI approach. *Journal of Process Control* 12: 3–13.

Ghosh A, Krishnan R and Subudhi B (2012) Robust PID compensation of an inverted cart-pendulum system: an experimental study. *IET Control Theory and Applications* 6: 1145–1152.

Goncalves EN, Palhares RM and Takahashi HC (2008) A novel approach for H_2 and H-infinity robust PID synthesis for uncertain systems. *Journal of Process Control* 18: 19–26.

Ho MT and Tu YW (2006) Position control of a single-link flexible manipulator using H-infinity based PID control. *IEE Proceedings: Control Theory and Applications*. Vol. 153; pp. 615–622.

Husain AR, Ahmad MN and Mohd Yatim AH (2008) Asymptotic stabilization of active magnetic bearing system using LMI-based sliding mode control. *International Journal of Mechanical System Science and Engineering* 2: 9–16.

Khairudin M, Mohamed Z, Husain AR and Ahmad MA (2010) Dynamic modelling and characterisation of a two-link flexible robot manipulator. *Journal of Low Frequency Noise, Vibration and Active Control* 29: 207–219.

Labibi B, Marquez J and Chen T (2011) LMI optimization approach to robust decentralized controller design. *International Journal of Robust and Nonlinear Control* 21: 904–924.

Li Y, Tang B, Shi Z and Lu Y (2000) Experimental study for trajectory tracking of a two-link flexible manipulator. *International Journal of Systems Science* 31: 3–9.

Li Y, Liu G, Hong T and Liu K (2005) Robust control of a two-link flexible manipulator with quasi-static deflection compensation using neural networks. *Journal of Intelligent and Robotic Systems* 44: 263–276.

Maxon Motor Ag Corporation (2003) *Maxon 03/04 the Leading Manufacturer of High Precision Drives and Systems*. Sachseln, Switzerland: Maxon Motor.

Morris AS and Madani A (1998) Quadratic optimal control of a two-flexible-link robot manipulator. *Robotica* 16: 97–108.

Olalla C, Leyva R, El Aroudi A, Garces P and Queinnec I (2010) LMI robust control design for boost PWM converters. *IET Power Electronics* 3: 75–85.

Pradhan SK and Subudhi B (2012) Real-time adaptive control of a flexible manipulator using reinforcement learning. *IEEE Transactions on Automation Science and Engineering* 9: 237–249.

Qiu Z, Han J and Liu J (2013) Experiments on fuzzy sliding mode variable structure control for vibration suppression of a rotating flexible beam. *Journal of Vibration and Control* Epub ahead of print 3 July 2013. DOI: 10.1177/1077546313487760.

Yin H, Kobayashi Y, Xu J and Huang F (2013) Theoretical and experimental investigation on decomposed dynamic control for a flexible manipulator based on nonlinearity. *Journal of Vibration and Control* Epub ahead of print 7 May 2013. DOI: 10.1177/1077546312474945.

Share

Journal of Vibration and Control

2015 Impact Factor: 1.643
2015 Ranking: 53/135 in Mechanics | 39/132 in Engineering, Mechanical | 10/32 in Acoustics
2016 Release of Journal Citation Reports, Source: 2015 Web of Science Data

Other Titles in:

Aerospace Engineering | Automotive Engineering | Civil Engineering

eISSN: 17412986 | ISSN: 10775463 | Current volume: 22 | Current issue: 20 Frequency: 16 Times/Year

Download flyer Recommend to Library

- Description
- Aims and Scope
- Editorial Board
- Abstracting / Indexing
- Submission Guidelines

ASSOCIATE EDITORS

EDITORIAL ADVISORY BOARD

Journal of Vibration and Control

Table of Contents

Volume 22, Issue 5, March 2016

Articles

A feedback chaotic image encryption scheme based on both bit-level and pixel-level

Guodong Ye, **Xiaoling Huang**

First Published August 25, 2015; pp. 1171–1180

› Show Abstract

A new method of updating mass and stiffness matrices simultaneously with no spillover

Jun Yang, **Huajiang Ouyang**, **Jia-Fan Zhang**

First Published May 19, 2014; pp. 1181–1189

› Show Abstract

Axial active magnetic bearing design

Gabriele Barbaraci

First Published May 13, 2014; pp. 1190–1197

› Show Abstract

Bifurcation behavior of steady vibrations of cantilever plates with geometrical nonlinearities interacting with three-dimensional inviscid potential flow

KV Avramov

First Published June 18, 2014; pp. 1198–1216

› Show Abstract

Nonlinear numerical model with contact for Stockbridge vibration damper and experimental validation

First Published May 19, 2014; pp. 1217–1227

› Show Abstract

Robustness studies of sensor faults and noises for semi-active control strategies using large-scale magnetorheological dampers

Young-Jin Cha, **Anil K Agrawal**

First Published May 21, 2014; pp. 1228–1243

› Show Abstract

Linear matrix inequality-based robust proportional derivative control of a two-link flexible manipulator

Z Mohamed, **M Khairudin**, **AR Husain**, **B Subudhi**

First Published June 18, 2014; pp. 1244–1256

› Show Abstract

Effects of delayed time active controller on the vibration of a nonlinear magnetic levitation system to multi excitations

Wedad A El-Ganaini, **Ali Kandil**, **Mustafa Eissa**, **Magdy Kamel**

First Published June 25, 2014; pp. 1257–1275

› Show Abstract

Study of radial vibrations in cylindrical bone in the framework of transversely isotropic poroelasticity

Malla Reddy Perati, **Sandhya Rani Bandari**

First Published June 25, 2014; pp. 1276–1287

› Show Abstract

Completely, partially centralized and fully decentralized control schemes of large adaptive mirrors

Mauro Manetti, **Marco Morandini**, **Paolo Mantegazza**

First Published June 30, 2014; pp. 1288–1305

› Show Abstract

Multi-objective optimization of actively controlled structures with topological considerations

Arjumand Ali, **Anoop K Dhingra**

First Published June 30, 2014; pp. 1306–1319

› Show Abstract

A vision-based vibration sensing and active control for a piezoelectric

First Published July 4, 2014; pp. 1320–1337

› Show Abstract

Shape memory alloy actuated structural control with discrete time sliding mode control using multirate output feedback

K Dhanalakshmi, **M Umapathy**, **D Ezhilarasi**

First Published July 4, 2014; pp. 1338–1357

› Show Abstract

Bifurcation results for a class of fractional Hamiltonian systems with Liouville–Weyl fractional derivatives

Nemat Nyamoradi, **Yong Zhou**

First Published July 25, 2014; pp. 1358–1368

› Show Abstract

Vibration study of non-homogeneous trapezoidal plates of variable thickness under thermal gradient

Arun Kumar Gupta, **Pragati Sharma**

First Published May 19, 2014; pp. 1369–1379

› Show Abstract

Propagation of Love waves in a heterogeneous medium over an inhomogeneous half-space under the effect of point source

Santimoy Kundu, **Shishir Gupta**, **Pramod Kumar Vaishnav**, **Santanu Manna**

First Published May 21, 2014; pp. 1380–1391

› Show Abstract

The nonlinear vibration and stability of a non-uniform continuous spindle system with nonlinear and nonsmooth boundaries

Shang-Han Gao, **Sheng-Long Nong**, **Wu-Bin Xu**, **Guang Meng**

First Published June 18, 2014; pp. 1392–1404

› Show Abstract

Vibration modeling of carbon-nanotube-based biosensors incorporating thermal and nonlocal effects

Kaifa Wang, **Baolin Wang**

First Published July 4, 2014; pp. 1405–1414

› Show Abstract

Kai Zhou, **Richard Christenson**, **Jiong Tang**

First Published June 30, 2014; pp. 1415–1430

› Show Abstract

A fault diagnosis approach for roller bearing based on improved intrinsic timescale decomposition de-noising and kriging-variable predictive model-based class discriminate

Yu Yang, **Haiyang Pan**, **Li Ma**, **Junsheng Cheng**

First Published July 4, 2014; pp. 1431–1446

› Show Abstract

Journal of Vibration and Control

ISSN: 1077-5463

Online ISSN: 1741-2986